

Document downloaded from:

<http://hdl.handle.net/10251/56864>

This paper must be cited as:

Camacho Torregrosa, F.J.; Pérez Zuriaga, AM.; Campoy Ungria, JM.; García García, A.; Tarko, A. (2015). Use of Heading Direction for Recreating the Horizontal Alignment of an Existing Road. *Computer-Aided Civil and Infrastructure Engineering*. 30(4):282-299. doi:10.1111/mice.12094.



The final publication is available at

<http://dx.doi.org/10.1111/mice.12094>

Copyright Wiley: 12 months

Additional Information

Use of Heading Direction for Recreating the Horizontal Alignment of an Existing Road

Francisco J. Camacho-Torregrosa, Ana M. Pérez-Zuriaga, José M. Campoy-Ungría, Alfredo García*

Highway Engineering Research Group (HERG), Universitat Politècnica de València, Spain

&

Andrew P. Tarko

Center for Road Safety, School of Civil Engineering, Purdue University, West Lafayette, Indiana, USA

Abstract: *This paper proposes a new method for fitting the horizontal alignment of a road to a set of (x, y) points. Those points can be obtained from digital imagery or GPS-data collection. Unlike current methods that represent road alignment through its curvature, the proposed method describes the horizontal alignment as a sequence of headings. An analytic-heuristic approach is introduced. The proposed method produces unique solutions even for complex horizontal alignments. Some examples and a case study are presented.*

This solution may not be accurate enough for road redesign, but it allows researchers and departments of transportation to obtain accurate geometric features.

1 INTRODUCTION

Road alignment recreation can be viewed as the process of fitting horizontal alignment curves to a sequence of points that represent the road centerline. The locations of points are typically measured with errors. Also, the design consistency of a road is evaluated with operating speed profiles estimated from the horizontal alignment parameters (e.g., the radii of circular curves). It sometimes becomes necessary to recreate the horizontal alignment of a road, for example, checking the design consistency of an existing road when its design documentation is not available or redesigning an existing road where a safety issue has been detected.

Although the points of the alignment can be known with relatively high accuracy, it may be necessary to recreate the components of the horizontal alignment (i.e., the parameters that represent the road's geometry in the design process that are subject to design decisions). The horizontal alignment of

a road is composed of the following three types of geometric components typically used by designers, which are subject to the existing standards:

- Tangents – straight segments with a zero curvature,
- Circular curves with a non-zero but constant curvature, and
- Clothoids (spiral transitions) that smoothly vary the curvature between the tangents and/or circular curves.

Some authors, such as Bosurgi and D'Andrea (2012) have investigated about the use of different curves instead of clothoids, due to better vehicle performance.

The process of recreating the road horizontal alignment is frequently conducted in two phases:

1. Measuring at certain frequency the locations of points along the road alignment and
2. Determining the geometric components of the alignment from the collected data points.

Several methods are available for the first step. Field surveying is one of the most accurate methods, but it is a high cost and time-consuming procedure, which limits its use for the mentioned applications. Another approach involves aerial imagery. Easa et al. (2007) and Dong et al. (2007) used IKONOS imagery for determining simple horizontal configurations of geometric elements. They first converted images from color to grayscale and then used the Canny edge detector to identify the road edges by detecting changes in the brightness level. This method is not as resource-demanding as topographic restitution, but it is less accurate and its accuracy depends on the quality of the images used. A different approach was performed by Tsai et al. (2010), who extracted roadway curvature data from photographic images. They proposed an algorithm that also used the Canny edge detector, thus automatically determining the location of

the centerline points of the road. They later were able to determine the radii of the different curves, although they were limited to horizontal curves with no spiral transitions.

GPS devices are also used for collecting road data points. Baffour et al. (1997) combined different GPS systems with vehicle data to obtain the road alignment, the longitudinal grades, and the superelevation rates. Roh et al. (2003) recreated several road alignments based on RTK DGPS (Real Time Kinematic Differential GPS) and GLONASS and studied their accuracy. Young and Miller (2005) developed methods capable of processing millions of data points collected by the Kansas Department of Transportation in the U.S. They also demonstrated that data points collected with GPS devices include an error term composed of constant and random components. The random error was found to be small, and the collected data were concluded to be useful for road geometry recreation.

Castro et al. (2006) presented another GPS-based technique of collecting road geometric data useful for recreating the geometry of the road centerline. They used a one-Hertz GPS receiver installed in a vehicle driven at 80 km/h. Pérez et al. (2010) used GPS devices placed on vehicles driven by regular drivers. They developed a method to determine the average vehicle path; and the results represent the average path followed by the drivers and not the road centerline. Such a horizontal line can be defined as the “operational alignment,” which is different from the designed alignment. The average behavior of both directions of travel should be considered. Its knowledge is also very useful due to its relationships to safety. Othman et al. (2012) also used a GPS-based naturalistic data collection method for developing a new procedure to identify horizontal curves.

Geographical Information System (GIS) maps are an efficient and fast way to deal with the horizontal alignment of roads (Shafahi and Bagherian, 2013). This is why several methods have been developed for working with GIS systems. Imran et al. (2006) used GPS and GIS systems for studying vehicle paths and recreating the horizontal alignment of roads. Cai and Rasdorf (2008) proposed a GIS- and LIDAR-based method for determining the centerlines of roads instead of using satellite imagery or GPS technology.

In the second phase of recreating the horizontal alignment, the sequence of the geometric components of the alignment that best fits the given set of points is determined. As the three types of geometric components are characterized by their curvature, most techniques analyze the profile of the road curvature. The curvature can be locally estimated by fitting a circle to three consecutive points. This procedure usually leads to a noisy and inconvenient curvature profile. Smoothing with user-defined thresholds is frequently required.

Cubic B-splines are often used to represent horizontal alignments; the continuity of these curves and their first derivatives make them convenient for that purpose. Ben-Arieh et al. (2004) and Castro et al. (2006) are among the

authors who fitted cubic B-splines to alignment data points. Cafiso and Di Graziano (2008) presented a method that deploys low-cost equipment to fit smoother splines to data points and to determine the road alignment parameters. However, there is a weakness in their approach, which is revealed if one attempts to use it to fit complex geometries. The splines-based approach seems to be applicable only to isolated curves or easy road geometry layouts. As demonstrated later in this paper, the curvature profile is also susceptible to errors caused by limited locations that sometimes make identification of the road geometric elements difficult.

Another approach to recreating road alignment involves user-defined thresholds for determining the break points between geometric components. Imran et al. (2006) used this approach, but they applied it to headings instead of curvatures. Their method first determines the heading direction for each point and assumes that the points that belong to a tangent section should have an “almost constant” heading direction. Thus, the difference between the heading directions of two consecutive points exceeding a certain threshold indicates the end of the tangent and the beginning of a different geometric component (e.g., a spiral transition or a circular curve). A horizontal curve is determined with the assumption that at least half of the points between two already identified consecutive tangents belong to a circular curve. A circular curve is fitted to these points and the fitting error is estimated. Then, two new adjacent points are added to the central section, and the circular curve is re-fitted with the corresponding error estimated. Expanding the circular curve is stopped when adding new points does not lead to a better solution. Next, the radius of the circular curve and the parameters of the spiral transitions are determined. Although finding the tangent sections by means of the heading direction is a good approach, a user-defined threshold must be used. Moreover, some curves may include fewer than half the points between two tangents, leading to a biased solution. This method works well if the geometry is relatively simple and composed of isolated curves. Othman et al. (2012) developed another procedure to determine the radius and the initial and final points of horizontal curves by using headings. They showed that headings lead to less noisy profiles than curvature-based profiles, such as the yaw rate. The radii of horizontal curves are estimated with a regression equation while the break points are determined based on thresholds established by the user.

There are some other methods that recreate the horizontal alignment from the (x, y) coordinates instead of using an indicator such as curvature or heading. The advantage of these approaches is that a better solution is normally achieved. On the other hand, only very simple geometries can be fitted, since the problem becomes very complex.

Easa et al. (2007) applied imagery data to recreate the horizontal alignment for circular curves and reverse curves without intermediate tangents. Based on some geometric

relationships, they were able to fit the best solution to the existing data by applying Hough's transformation. This method was applied on raster images and identified the pixels belonging to each element. This method was further improved by Dong et al. (2007), adding the possibility of determining the radii and parameters for circular curves with symmetric transition curves. These methodologies produced a very high level of accuracy, but its applications are limited to the geometric cases included in their research.

There are some additional methods for calculating curve radii based on few points. These methodologies are very useful when data is extracted from GIS, but they are normally limited to circular curves with no spiral transitions (Hummer et al., 2010). Price (2010) proposed a method for determining the curve radii from GIS data by means of using the Middle Ordinate (i.e., the perpendicular distance from the chord to the maximum curve extent). Li (2012) proposed a method and an add-in tool in ArcMap for identifying simple curves from GIS data. However, both approaches were only valid for simple geometries with no spiral transitions.

Hans et al. (2012) developed a GIS-based horizontal alignment recreation method for determining the radii of horizontal curves and their relationship to safety. Their method was based on determining the properties of the circular curves by means of comparing the results of two techniques: circular regression and Newton iteration of the

modified circular curve equation. However, this was also limited to circular curves with no spiral transitions.

Camacho et al. (2010) developed a method for obtaining an improved curvature profile for the alignment passing a set of points collected with the low-cost data collection technique applied by Pérez et al. (2010). The method considers more than three points for estimating curvature; and additional smoothing processes were introduced to improve the accuracy. Compared to other methods, the alignment components are easily distinguishable in the obtained "raw curvature profile." The final sequence of tangents, circular curves, and spiral transitions are produced with a user-defined thresholds procedure. Figure 1a shows a raw curvature profile and several results obtained for different thresholds. The smoothing process may have slightly affected the alignments. Figure 1b shows the final adjusted profile.

2 OBJECTIVES AND PAPER ORGANIZATION

A new low-cost method of fitting horizontal alignment to a set of 2D points (orthogonal projection of 3D data points on a horizontal plane) is presented in this paper. The proposed method addresses some of the most important problems of the current methods discussed above. This new method uses the heading direction to represent the horizontal alignment of the road.

The "Basic Considerations" section discusses the effect of the point location error on the "noisiness" of the road alignment representation via curvatures and headings. Then, a representation of the design curves (tangent, circular curve, and spiral transition) as a sequence of headings is described and a formulation of the general optimization problem is presented. The advantages of the heading method also are discussed.

The "Heuristic Approximation" section considers the theoretical fundamentals of the method and proposes several heuristic algorithms for fitting different sequences of horizontal geometric elements. A computer program including all the algorithms also is introduced.

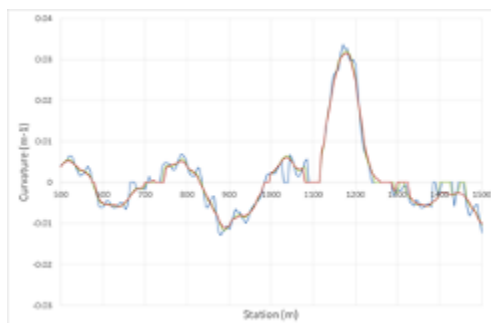
The advantages of the proposed method with examples are presented in the "Discussion" section; and the paper then concludes with a summary the method and identification of further research needs.

The computer program in the proposed method was developed with Visual Basic for Applications embedded in Microsoft Office Excel. All the examples shown were obtained using this program.

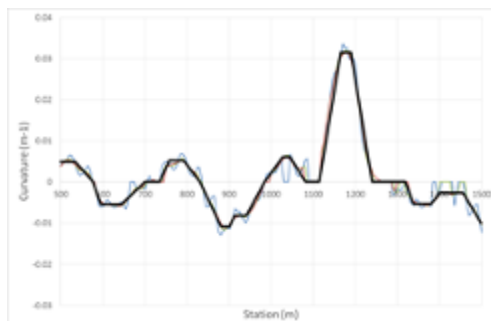
3 BASIC CONSIDERATIONS

3.1. Data source

The initial set of point locations must be in the Cartesian system (x, y coordinates), which may be obtained in several ways. GPS-equipped vehicles can be used for determining



Selected Road Segment (st. 500 - 1500 m)



Estimated Alignment of the Selected Road Segment

Figure 1 Curvature-based fitting of a horizontal alignment.

the typical vehicle paths, called sometimes “operating paths.” Nowadays, the locations of designed and existing roads are typically available on electronic maps and orthogonal images with embedded geo-coordinates. Therefore, the geo-coded locations of the centerline road point sequence can be obtained by the user manually from such maps and aerial imagery. In many cases of existing roads, design documentation does not exist or retrieving the paper-based design documentation is not practical when an alternative of high quality orthogonal and geo-coded images are available. Therefore, a method of estimating the curvature profile is needed and, more specifically, such a method should estimate a complete set of design parameters from the (x, y) data extracted from images. In a general case, a sequence of (x, y) data points may follow the centerline of the road, the centerline of a selected traffic lane, or the edge of a lane. Some advanced methods, such as those presented in the literature review can also be used for determining the road centerline.

3.2 Consideration of the location error

Determining the geometric elements that compose the horizontal alignment of a road from a set of data points is not easy. As revealed by our literature review, the first approach to this task utilized an initial curvature profile estimated from the points. A curvature profile (s, κ) is used in road designing to depict the rate κ at which the road changes its direction per the unit distance (curvature $\kappa=1/R$) at any point along the road at distance s from the beginning (station s). Unlike the (x, y) road alignment, the curvature profile (s, κ) is not smooth and even may not be continuous. It is composed of horizontal lines with $\kappa=0$ that represent tangents, horizontal lines with $\kappa \neq 0$ that represent circular curves, and sloped straight lines that represent spiral transitions. Such a profile was meant to help identify the presence of spirals and compound circular curves.

The proposed heading profile is related to curvature in the following way:

$$\kappa = \frac{d\theta}{ds} \quad (1)$$

where:

- κ : Curvature (m^{-1}),
- θ : Heading (rad),
- s: Distance (m).

The following section discusses the level of noise (random error) expected in the curvature and headings profiles under certain assumptions to demonstrate which profile is a more convenient representation of the road alignment. The noise level is measured with the standard deviation of the random error compared to the minimum changes in the profile values that ought to be detectable.

An extraction of point location data from the alignment yields a sequence of (x, y) coordinates. These coordinates

can be converted to the corresponding initial heading profile (s, θ) by calculating Δs and θ with the following equations:

$$\Delta s_i = \sqrt{\Delta x_i^2 + \Delta y_i^2} \quad (2)$$

$$\theta_i = \begin{cases} \arctan\left(\frac{\Delta y_i}{\Delta x_i}\right) & ; \Delta x_i \neq 0 \\ \pm \frac{\pi}{2} & ; \Delta x_i = 0 \end{cases} \quad (3)$$

where:

coordinates (x_i, y_i) represent point i located at distance s_i from the beginning of the alignment

$$\Delta x_i = x_{i+1} - x_i,$$

$$\Delta y_i = y_{i+1} - y_i.$$

The initial curvature profile (s, κ) can be determined by estimating the radius R of a circular curve that passes through three consecutive points and calculating the corresponding curvature $\kappa=1/R$ assigned to the middle point with station s. Another option, used here, is to calculate curvature κ with Equation 1. The increment of road length ds is approximated with the length of a short segment calculated with Equation 2, and the change of the heading $d\theta$ is approximated with the change in the headings of the two consecutive short segments. The latter method leads to the following calculation of the curvature at station s_i :

$$\kappa_i = \frac{\theta_{i+1} - \theta_i}{\Delta s_i} \quad (4)$$

The primary objective when extracting location data is reducing the lateral error to the maximum extent while keeping the longitudinal separation of points constant. Thus, it is more relevant and convenient to discuss the data location errors in terms of longitudinal and lateral errors. Let us assume that the longitudinal separations along the alignment are, on average, m_s with a limited standard deviation of these separations σ_s . The lateral error e_l is the distance between the estimated location of a point and the actual road alignment. Their mean value is zero and their standard deviation is σ_l .

A successful identification of individual curves, or more precisely, changes in the curvature caused by the presence of these curves is possible if the error in the curvature estimates is considerably lower than these changes. To test this condition, let us consider the standard estimation error $\sigma_{\Delta\theta}$ of changes in θ and $\sigma_{\Delta\kappa}$ in κ . The standard deviation of separation is kept much smaller than its mean value m_s . This assumption allows stating that $e_\theta \cong e_l/m_s$. Another assumption is that the lateral error e_l is i.i.d. (independent and identically distributed) and normally distributed. This assumption is valid if the point data are collected by human observers from paper documentation or from digital renderings of the alignment. Although GPS data may exhibit serial correlation and the i.i.d. assumption does not hold in this case, the findings from the following analysis should also be applicable also to GPS data.

Table 1
Location error versus ability to identify curves in horizontal alignments.

Lateral standard error (m)	Alignment points interval Δs (m)	Headings profile		Curvature profile	
		Std. error of θ change estimate (rad)	Minimum detectable change in heading (°)	Std. error of κ change estimate (1/m)	Largest radius of detectable isolated curve (m)
0.02	2	0.0141	1.6	0.01000	50 x
0.02	5	0.0057	0.64	0.00160	312 x
0.02	10	0.0028	0.3	0.00040	1250
0.05	2	0.0354	4.1 x	0.02500	20 x
0.05	5	0.0141	1.6	0.00400	124 x
0.05	10	0.0071	0.83	0.00100	500 ?

Notes: Symbol ? indicates profiles that are noisy enough to make identifying flat horizontal curves difficult.

Symbol x indicates profiles so noisy that identifying most of horizontal curves is quite difficult.

The approximation $e_\theta \cong e_l/m_s$ and the assumption of i.i.d. for the e_l error allow calculating the standard error of the change in the heading as

$$\sigma_{\Delta\theta} = \frac{\sqrt{2}}{m_s} \cdot \sigma_l \quad (5)$$

Equation 4 can be approximated with $\kappa = \Delta\theta/m_s$, thus the standard error of κ estimate is $\sigma_\kappa = \sigma_{\Delta\theta}/m_s$ or $\sigma_\kappa = \sqrt{2}e_l/m_s^2$. Using the i.i.d. assumption again, this time for the e_κ error, the following can be stated for the standard error of the curvature change:

$$\sigma_{\Delta\kappa} = \frac{2}{m_s^2} \cdot \sigma_l \quad (6)$$

Table 1 presents the standard errors in the estimates of the headings changes and curvature changes calculated for any two consecutive points of the horizontal alignment. The corresponding detectable changes in the headings and curvature profiles are also provided. They are assumed to be twice the estimation standard error. The table clearly indicates that, in the majority of cases, the curvature profiles are too “noisy” to allow convenient identification and estimation of curves. On the other hand, the heading profile is less “noisy,” and even small changes in the headings can be conveniently detected.

Another consideration of the location error is its impact on the accuracy of s in the estimated curvature and heading profile. Since the Δs calculated with Equation 2 is not measured exactly along the alignment but rather along a line that tends to be at a slight skew to the alignment due to the lateral errors e_l , the distance s is overestimated and this overestimation is growing with distance. Fortunately, the longitudinal error e_s is negligible when evaluating the driving convenience and safety. For example, a statistical simulation that followed the stated earlier assumptions has shown that a point one kilometer away from the beginning is expected to

be shifted by approximately 0.35 m if the data points on the alignment are separated by two meters and the lateral location accuracy is 0.02 m (standard deviation). This overestimation may require adjustments if the reconstructed location of the alignment is important.

It can be concluded that, to produce good results, the alignment points separated by two meters ($\Delta s=2$ m) should not have the standard measurement error exceeding 0.02 meter. This paper shows how to utilize heading profiles to fit horizontal alignments to data points obtained from manual image-based data collection. Another data collection method previously discussed uses drivers’ paths. Camacho et al. (2010) developed a method that combines different paths followed by drivers into a single one called the “average path” with the alignment points separated at 1 m.

3.3 Components of horizontal alignment

The horizontal curvature of a road strongly affects the safety and comfort of travel, and that is why curvature profiles are widely used in road design and road alignment analysis. Three kinds of geometric elements are used in designing the horizontal alignment of roads: tangents, circular curves, and spiral transitions. These are the components that closely follow the natural vehicle paths, and the existing design standards apply to the parameters of these curves. Each type of curve has a distinct curvature profile shape.

A horizontal alignment is normally composed of a series of tangents separated by curves. These curves may or may not present spiral transitions. The proposed new method covers all these situations, but does not consider curve-to-curve transitions (with or without spiral transitions). The last case has also been developed, but it is not presented due to the brevity required here and because it is rare in that it is mainly used in loops and odd geometries. However, it will be presented in further publications.

Table 2
Curvature-heading correspondences.

Geometric element	Curvature	Heading
Tangent	$\kappa = 0$	$\theta = \int 0 \cdot ds = \theta_k$
Circular curve	$\kappa = c_k$	$\theta = \int c_k \cdot ds = c_k \cdot s + \theta_k$
Spiral transition	$\kappa = \frac{s + d_0}{A^2}$	$\theta = \int \frac{s + d_0}{A^2} \cdot ds = \frac{1}{A^2} \cdot \left[\frac{s^2}{2} + d_0 \cdot s + \theta_k \right]$

κ : Curvature (m^{-1}), θ : Heading (centesimal degrees),
 s : Distance measured from the beginning of the geometric element (m),
 A : Parameter of the spiral transition (m), d_0, c_k, θ_k : Constants

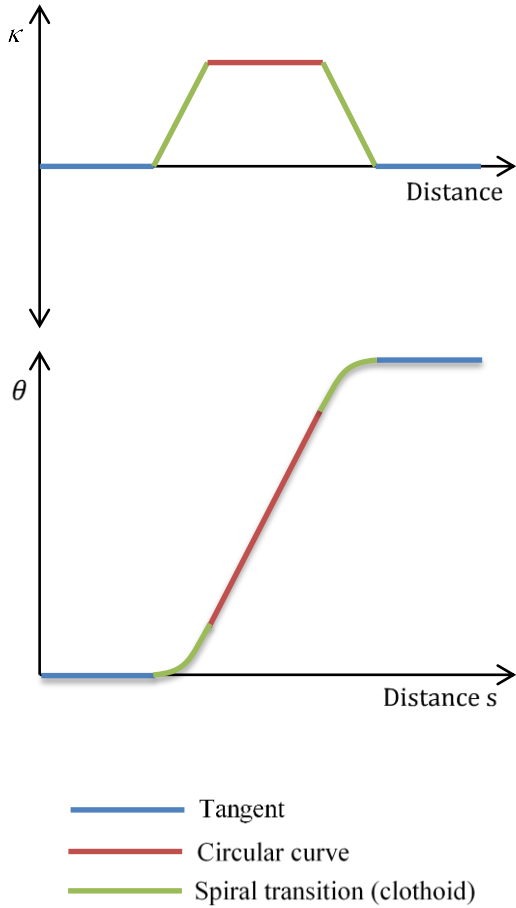


Figure 2 A horizontal curve expressed in terms of curvature κ and heading direction θ

Analyzing the horizontal alignment based on the heading profile instead of the curvature profile presents two important advantages:

- As demonstrated above, the heading profile is considerably less sensitive to measurement error, which allows the alignment components to be easily identifiable, even including visual inspection by the user. This benefit is clear when comparing the heading profile to the curvature profile.

- The road heading must always be continuous. This means that the heading value presented by a geometric element at its final point must always be the same as the initial heading value of the following geometric element. Consequently, fitting the alignment in this way allows sharing some information longitudinally, thereby addressing some issues produced by the randomness of the data. Moreover, in most cases the heading's first derivative is also continuous (except when a large radius of the circular curve eliminates the necessity of using spiral transitions), meaning that a continuity in the heading's slope profile must also be satisfied, thus adding more information. The curvature profile does not present this property, and the different geometric elements must be independently fitted, producing less accurate solutions.

For the reasons previously explained, the heading profile will be used to represent the horizontal alignment. Table 2 shows the relationships between the station s and the curvature κ and heading θ for tangents, circular curves, and spiral transitions. Figure 2 shows example profiles of curvature (Figure 2a) and heading (Figure 2b) for a single horizontal curve with spiral transitions and tangent sections and a heading direction. Tangents, circular curves, and spiral transitions are horizontal, sloped, and parabolic lines on the heading profile, respectively.

3.4 General formulation and solution of the problem

The horizontal alignment recreation problem can be described in general terms as fitting the three types of alignment components by minimizing the square-mean error of heading estimates while preserving the continuity of the heading at the stitching points between the geometric elements. The continuity of the heading's first derivative (curvature) must also be preserved if the transition curves are used. The decision variables include the parameters of the alignment curves and the stitching points. The continuity conditions are the constraints of the problem. Table 2 shows that a tangent heading curve has one parameter, a circular curve – two, and a transition curve – three.

To simplify the problem, it is assumed that the number and type of curves of the sequence are known. This

requirement can be partly relaxed by assuming that at least the number of tangents is known, and only one circular curve between two consecutive tangents is allowed (no compound curves), which is valid for the vast majority of horizontal geometric layouts. The presence of transition curves at the end of each circular curve is also assumed.

The problem is a mixed integer optimization problem. There are a limited number of discrete positions for the stitching points. On the other hand, knowing the stitching points allows fitting individual heading curves that are continuous functions. The general strategy is to separate the integer and continuous problems by solving them interchangeably until the solution converges. Fortunately, when the stitching points are known (or solved), the number of constraints and decision variables can be made equal in all cases. Thus, only one set of curves exists that meets the continuity and smoothness conditions. These curves can be easily calculated from the system of linear equations that represents the continuity and smoothness conditions at the stitching points.

The overall solving strategy includes:

- (1) Balancing the number of curve parameters with the number of continuity/smoothness conditions.
- (2) Solving the system of linear equations to obtain feasible curves for the current stitching points.
- (3) Finding the best stitching points for the current set of curves.
- (4) Repeating steps 2 and 3 until the solution converges.

Decomposition of the entire problem by dividing the alignment into shorter pieces is another strategy used to simplify and speed up the search for the solution. The midpoints of tangent segments are the natural choice, which reduces the number of tangents in each sub-problem to two and the number of circular curves to one (no compound curves). After solving all the sub-problems, the entire

alignment can be obtained by combining the solutions of sub-problems.

The following section discusses selected cases in a more specific and analytical manner. A heuristic procedure of finding the best stitching points is also presented and demonstrated with examples.

4 HEURISTIC APPROXIMATION

This section develops the methodology for different geometric sequences, considering the equations, the continuity conditions, and the heuristic process. Although the analytical solution is always valid, the heuristic process has been programmed to work with a set of points regularly separated at a one meter interval ($\Delta s = 1$ m).

4.1 A single circular curve with spiral transitions

Figure 3 shows the particular solution to an isolated curve, composed of tangent T_1 – spiral transition Cl_1 – circular curve C – spiral transition Cl_2 – tangent T_2 . The user has to detect two points belonging to the initial and final tangents (it does not matter where they are located as long as they belong to the corresponding tangent). These points are known as x_0 and x_5 . There are more x_i stitching points (with i ranging from 1 to 4) between each one of the different road geometric elements.

$$\text{Tangent } T_1: \theta_{T_1} = c_1 \tag{7}$$

$$\text{Spiral transition } Cl_1: \theta_{Cl_1} = a_2 \cdot s^2 + b_2 \cdot s + c_2 \tag{8}$$

$$\text{Circular curve } C: \theta_C = b_3 \cdot s + c_3 \tag{9}$$

$$\text{Spiral transition } Cl_2: \theta_{Cl_2} = a_4 \cdot s^2 + b_4 \cdot s + c_4 \tag{10}$$

$$\text{Tangent } T_2: \theta_{T_2} = c_5 \tag{11}$$

At all stitching points, the heading and curvature continuity must be satisfied:

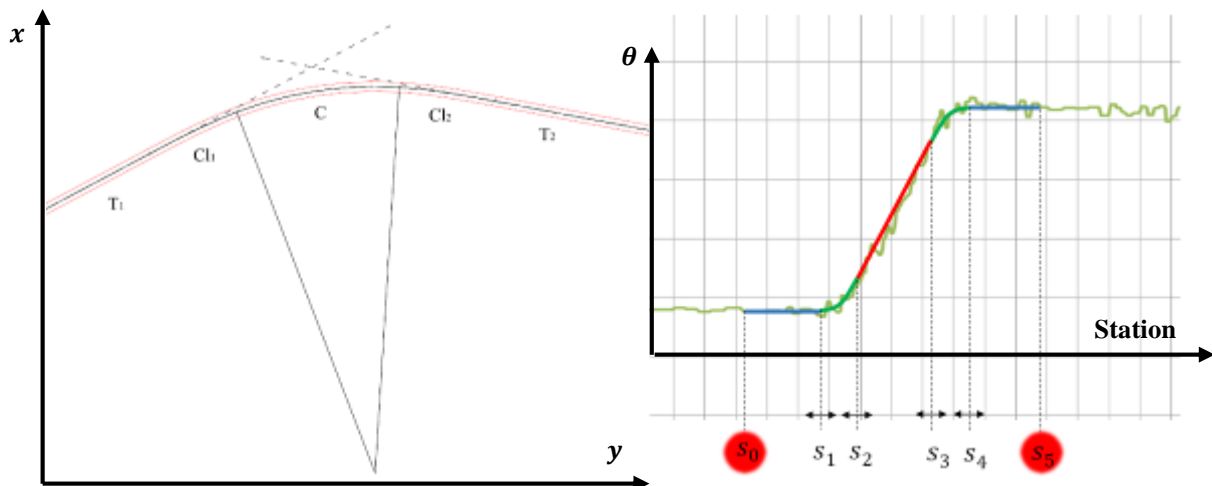


Figure 3 Geometric layout and heading profile for an isolated curve.

$$\begin{cases} \lim_{s \rightarrow s_i^-} \theta(s_i) = \lim_{s \rightarrow s_i^+} \theta(s_i) \\ \lim_{s \rightarrow s_i^-} \theta'(s_i) = \lim_{s \rightarrow s_i^+} \theta'(s_i) \end{cases} \quad (12)$$

Being s_i the stitching points, where $i = 1$ to 4.

Hence, eight conditions can be obtained:

- Point s_1 :

$$\text{Heading: } \theta_{T_1}(s_1) = \theta_{Cl_1}(s_1) \rightarrow c_1 = a_2 \cdot (13)$$

$$s_1^2 + b_2 \cdot s_1 + c_2$$

$$\text{Curvature: } \theta'_{T_1}(s_1) = \theta'_{Cl_1}(s_1) \rightarrow 0 = 2 \cdot a_2 \cdot (14)$$

$$s_1 + b_2$$

- Point s_2 :

$$\text{Heading: } (15)$$

$$\theta_{Cl_1}(s_2) = \theta_C(s_2) \rightarrow a_2 \cdot s_2^2 + b_2 \cdot s_2 + c_2 = b_3 \cdot$$

$$s_2 + c_3$$

$$\text{Curvature: } (16)$$

$$\theta'_{Cl_1}(s_2) = \theta'_C(s_2) \rightarrow 2 \cdot a_2 \cdot s_2 + b_2 = b_3$$

- Point s_3 :

$$\text{Heading: } (17)$$

$$\theta_C(s_3) = \theta_{Cl_2}(s_3) \rightarrow b_3 \cdot s_3 + c_3 = a_4 \cdot s_3^2 + b_4 \cdot$$

$$s_3 + c_4$$

$$\text{Curvature: } (18)$$

$$\theta'_C(s_3) = \theta'_{Cl_2}(s_3) \rightarrow b_3 = 2 \cdot a_4 \cdot s_3 + b_4$$

- Point s_4 :

$$\text{Heading: } (19)$$

$$\theta_{Cl_2}(s_4) = \theta_{T_2}(s_4) \rightarrow a_4 \cdot s_4^2 + b_4 \cdot s_4 + c_4 = c_5$$

$$\text{Curvature: } (20)$$

$$\theta'_{Cl_2}(s) = \theta'_{T_2}(s_4) \rightarrow 2 \cdot a_4 \cdot s_4 + b_4 = 0$$

There is a lack of two equations since the system is composed by eight equations and there are ten unknown parameters. The OLS (Ordinary Least Squares) estimation of the headings is sufficient if the lateral location errors e_l are indeed i.i.d. and normally distributed. This is not a problem because θ_{T_1} and θ_{T_2} (heading direction of the initial and final tangents) can be determined from the simple calculation of the average values within the currently tangent ranges (Equations 21 and 22). No weighting is needed if the separations between points are approximately equal.

$$\theta_{T_1} = \frac{\sum_{s=s_0}^{s=s_1} \theta(s)}{(s_1 - s_0)} \quad (21)$$

$$\theta_{T_2} = \frac{\sum_{s=s_4}^{s=s_5} \theta(s)}{(s_5 - s_4)} \quad (22)$$

Thus, there are eight unknown variables and eight equations. The system can now be solved. Equations 23 to

30 show the expressions for each one of the corresponding coefficients.

$$a_2 = \frac{\theta_{T_1} - \theta_{T_2}}{((s_1 + s_2) - (s_3 + s_4))(s_2 - s_1)} \quad (23)$$

$$b_2 = \frac{2(\theta_{T_2} - \theta_{T_1})s_1}{((s_1 + s_2) - (s_3 + s_4))(s_2 - s_1)} \quad (24)$$

$$c_2 = \theta_{T_1} + \frac{(\theta_{T_1} - \theta_{T_2})s_1^2}{((s_1 + s_2) - (s_3 + s_4))(s_2 - s_1)} \quad (25)$$

$$b_3 = \frac{2(\theta_{T_1} - \theta_{T_2})}{(s_1 + s_2) - (s_3 + s_4)} \quad (26)$$

$$c_3 = \frac{\theta_{T_2}(s_1 + s_2) - \theta_{T_1}(s_3 + s_4)}{(s_1 + s_2) - (s_3 + s_4)} \quad (27)$$

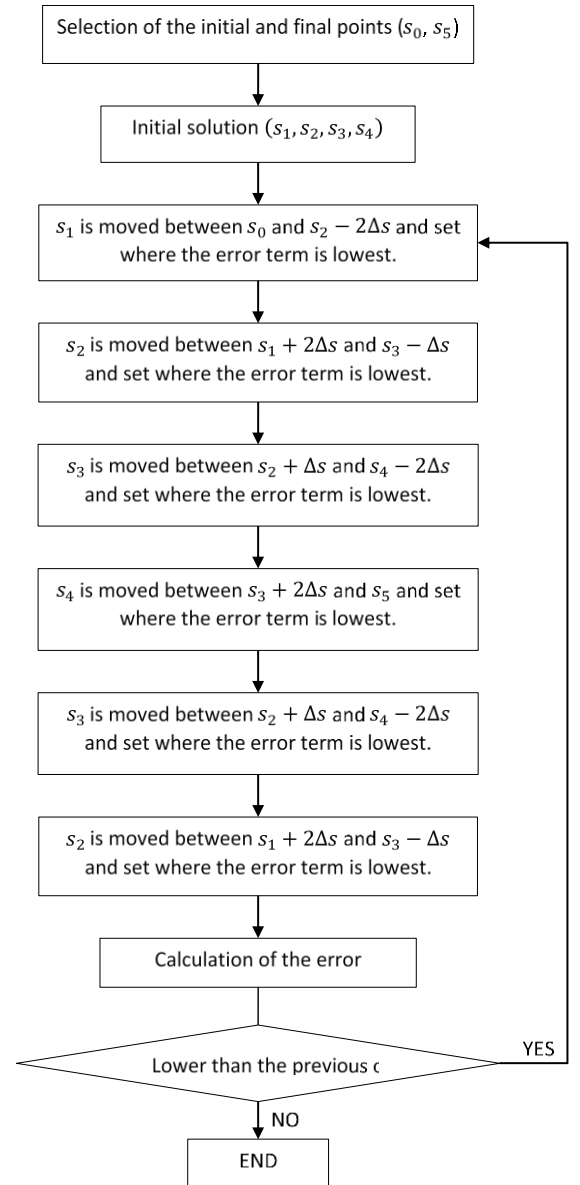


Figure 4 Flowchart for fitting an isolated curve.

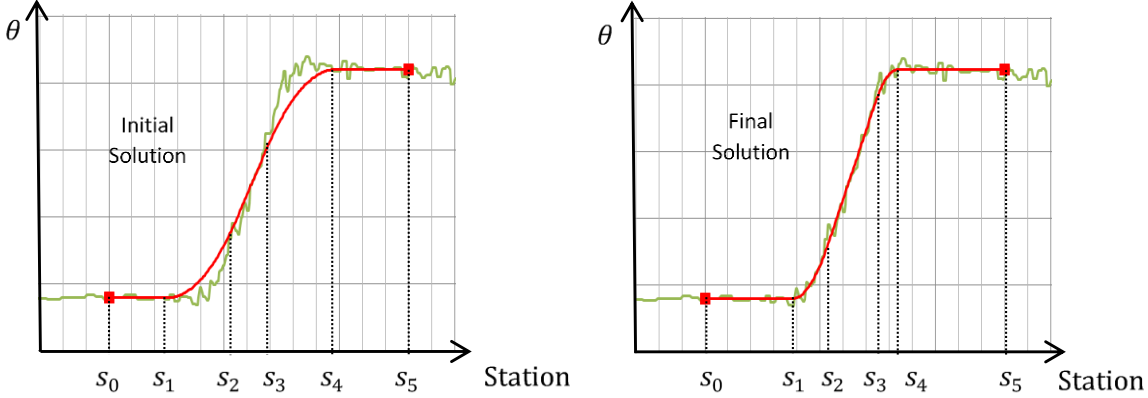


Figure 5 Isolated curve adjustment: initial and final solutions.

$$a_4 = \frac{\theta_{T_1} - \theta_{T_2}}{((s_1 + s_2) - (s_3 + s_4))(s_3 - s_4)} \quad (28)$$

$$b_4 = \frac{2(\theta_{T_2} - \theta_{T_1})s_4}{((s_1 + s_2) - (s_3 + s_4))(s_3 - s_4)} \quad (29)$$

$$c_4 = \theta_{T_2} + \frac{(\theta_{T_1} - \theta_{T_2})s_4^2}{((s_1 + s_2) - (s_3 + s_4))(s_3 - s_4)} \quad (30)$$

A heuristic approximation is now required to determine the $s_1 \dots s_4$ combination that gives the best solution to the problem. For each individual solution, the error term (E) between the initial heading profile (θ_0) and the fitted one (θ) is given by Equation 31.

$$E = \frac{\sum_{s=s_0}^{s=s_5} (\theta(s) - \theta_0(s))^2}{s_5 - s_0} \quad (31)$$

The final location of each stitching point will be the one which leads to the general solution with the lowest error. This solution depends on the position of all these points; therefore, they cannot be fitted one by one. A heuristic method was developed in order to obtain the final solution. Figure 4 summarizes this process.

The stitching points must be ordered and keep some distance for computing purposes (no distance needed for tangents, Δs for circular curves and $2\Delta s$ for spiral transitions). These conditions for the heuristic process are:

- s_1 varies from s_0 to $s_2 - 2\Delta s$.
- s_2 varies from $s_1 + 2\Delta s$ to $s_3 - \Delta s$
- s_3 varies from $s_2 + \Delta s$ to $s_4 - 2\Delta s$
- s_4 varies from $s_3 + 2\Delta s$ to s_5

After a number of iterations, the best solution is reached.

Figure 5 shows one of the initial solutions and the final one. Note that the user only had to select two points belonging to the consecutive tangents. It is not required that these points coincide with the beginning (or ending) of the tangents. Furthermore, it is recommended that the user select

a large portion of the tangents in order to get a better approximation to their actual heading directions. Since the tangent heading is easy to estimate, any reasonable selection of tangent points used in the estimation produces a good result. Both spiral transitions are not forced to be similar.

4.2 A single circular curve without spiral transitions

Flat circular curves do not require spiral transitions. In this case, the previous solution for curves with spirals can be used if one assumes spirals with minimal lengths (each $2\Delta s$ long). This approximation is acceptable for a practical purpose. An exact solution with no spiral transitions can be obtained if the number of equations and the parameters remain the same. In this case, there is continuity of the heading direction, but not for its first derivative. Hence, the number of equations for each stitching point is reduced to one. On the other hand, the number of stitching points is reduced to two (preceding tangent to circular curve and circular curve to following tangent).

The heading direction for each one of the road geometric elements is:

$$\text{Tangent } T_1: \theta_{T_1} = c_1 \quad (32)$$

$$\text{Circular curve } C: \theta_C = b_2 \cdot s + c_2 \quad (33)$$

$$\text{Tangent } T_2: \theta_{T_2} = c_3 \quad (34)$$

In this case, only the continuity condition has to be satisfied at the stitching points (s_1 and s_2):

$$\lim_{s \rightarrow s_1^-} \theta(s_i) = \lim_{s \rightarrow s_1^+} \theta(s_i) \quad (35)$$

Two conditions must be satisfied:

- Point s_1 :

$$\text{Heading: } \theta_{T_1}(s_1) = \theta_C(s_1) \rightarrow c_1 = b_2 \cdot s_1 + c_2 \quad (36)$$

- Point s_2 :

$$\text{Heading: } \theta_C(s_2) = \theta_{T_2}(s_2) \rightarrow b_2 \cdot s_2 + c_2 = c_3 \quad (37)$$

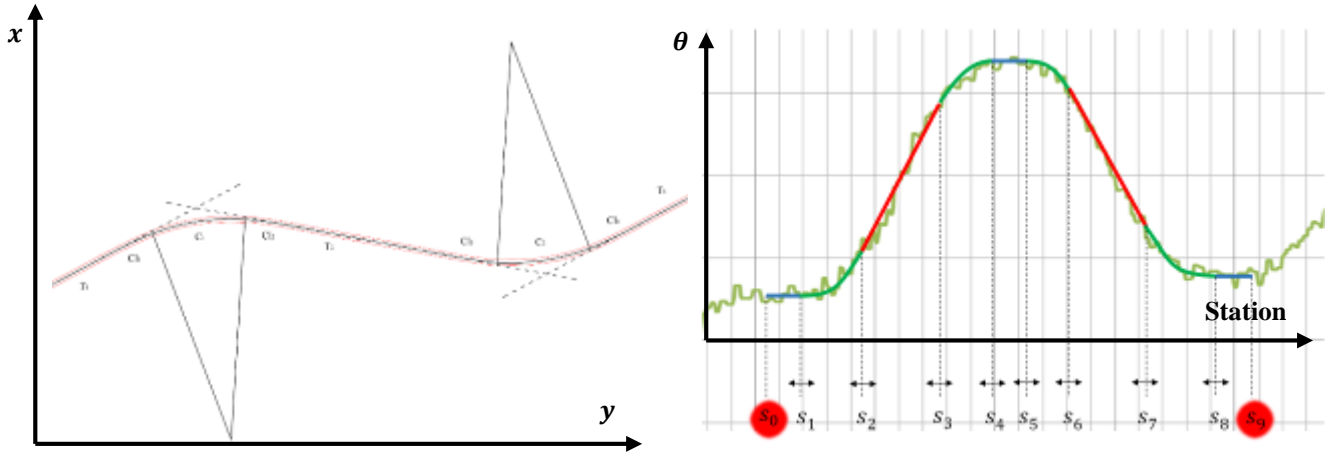


Figure 6 Geometric layout and heading profile for reverse and broken back curves ($n=2$).

Again, parameters c_1 and c_3 are already known since they are the fitted heading direction of the preceding (θ_{T_1}) and the following (θ_{T_2}) tangents, respectively. The solution of the system is:

$$b_2 = \frac{c_3 - \theta_{T_1}}{s_2 - s_1} \quad (38)$$

$$c_2 = \theta_{T_1} - \frac{\theta_{T_2} - \theta_{T_1}}{s_2 - s_1} \cdot s_1 \quad (39)$$

The proposed procedure starts with fitting an isolated curve with spirals to the alignment points. If the solution converges to the minimum spirals of with the minimum length, the case without spirals is solved next. Out of the two obtained solutions, the solution with a smaller estimation error calculated with Equation 31 is selected as the final one.

4.3 Sequence of circular curves

The previously discussed cases require distinguishable tangent segments that separate the curves from each other. Sometimes, the horizontal alignment is composed of a series of several curves with almost negligible tangents. In this case, it is not easy for the user to identify points that belong to tangents.

The previous cases can be expanded in order to fit several curves at the same time if the number of equations (constraints) equals the number of parameters to be estimated. The main advantage of this procedure, compared to fitting each curve separately, is that the program converges to the most accurate position of the intermediate tangents, even if their lengths are short. The case of no tangent between curves is also included as a feasible solution.

The general approach is the same as in the previous cases, although the heuristic process has to consider $4n$ boundary points, n being the number of circular curves (Figure 6). The number of resulting equations from the boundary points is $8n$ (two for each point). With i being each one of the circular curves, ranging from 1 to n , the expressions of the

corresponding geometric elements can be expressed in a matrix form (Equation 40).

The stitching points for a curve i are the following:

- Tangent T_i : from s_{4i-4} to s_{4i-3} .
- Spiral transition Cl_{2i-1} : from s_{4i-3} to s_{4i-2} .
- Circular curve C_i : from s_{4i-2} to s_{4i-1} .
- Spiral transition Cl_{2i} : from s_{4i-1} to s_{4i} .

$$\begin{pmatrix} \theta_{T_1} \\ \theta_{Cl_1} \\ \theta_{C_1} \\ \theta_{Cl_2} \\ \theta_{T_2} \\ \theta_{Cl_3} \\ \theta_{C_2} \\ \theta_{Cl_4} \\ \dots \\ \theta_{T_i} \\ \theta_{Cl_{2i-1}} \\ \theta_{C_i} \\ \theta_{Cl_{2i}} \\ \dots \\ \theta_{T_n} \\ \theta_{Cl_{2n-1}} \\ \theta_{C_n} \\ \theta_{Cl_{2n}} \\ \theta_{T_{n+1}} \end{pmatrix} = \begin{pmatrix} 0 & 0 & c_1 \\ a_2 & b_2 & c_2 \\ 0 & b_3 & c_3 \\ a_4 & b_4 & c_4 \\ 0 & 0 & c_5 \\ a_6 & b_6 & c_6 \\ 0 & b_7 & c_7 \\ a_8 & b_8 & c_8 \\ \dots & \dots & \dots \\ 0 & 0 & c_{4i-3} \\ a_{4i-2} & b_{4i-2} & c_{4i-2} \\ 0 & b_{4i-1} & c_{4i-1} \\ a_{4i} & b_{4i} & c_{4i} \\ \dots & \dots & \dots \\ 0 & 0 & c_{4n-3} \\ a_{4n-2} & b_{4n-2} & c_{4n-2} \\ 0 & b_{4n-1} & c_{4n-1} \\ a_{4n} & b_{4n} & c_{4n} \\ 0 & 0 & c_{4n+1} \end{pmatrix} \cdot \begin{pmatrix} s^2 \\ s \\ 1 \end{pmatrix} \quad (40)$$

Each curve adds nine unknown variables, and the last tangent adds an additional one. Hence, the number of unknown parameters is $9n + 1$. However, the tangent-related parameters are known since they can be directly obtained once the position of their stitching points is defined. This eliminates $n + 1$ parameters of the equation system and the final number of unknowns being $8n$, which is the same

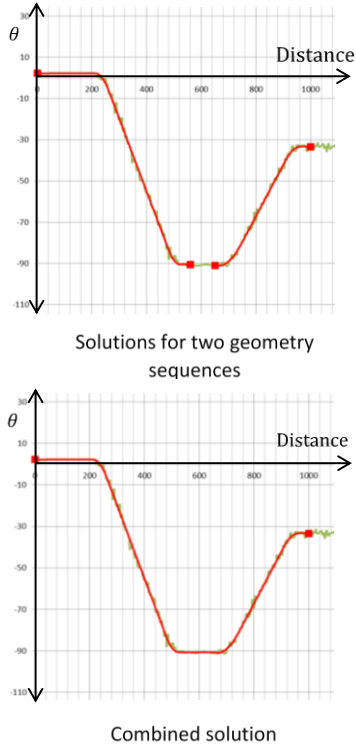


Figure 7 Combining solutions by removing gaps between fitted alignments inside tangents.

as the number of equations. This allows us to generate a system to solve the parameters. The solution to the problem is shown in the following equations, for i from 1 to n :

$$a_{4i-2} = \frac{\theta_{T_i} - \theta_{T_{i+1}}}{((s_{4i-3} + s_{4i-2}) - (s_{4i-1} + s_{4i}))(s_{4i-2} - s_{4i-3})} \quad (41)$$

$$b_{4i-2} = \frac{2(\theta_{T_{i+1}} - \theta_{T_i})s_{4i-3}}{((s_{4i-3} + s_{4i-2}) - (s_{4i-1} + s_{4i}))(s_{4i-2} - s_{4i-3})} \quad (42)$$

$$c_{4i-2} = \theta_{T_i} + \frac{(\theta_{T_i} - \theta_{T_{i+1}})s_{4i-3}^2}{((s_{4i-3} + s_{4i-2}) - (s_{4i-1} + s_{4i}))(s_{4i-2} - s_{4i-3})} \quad (43)$$

$$b_{4i-1} = \frac{2(\theta_{T_i} - \theta_{T_{i+1}})}{(s_{4i-3} + s_{4i-2}) - (s_{4i-1} + s_{4i})} \quad (44)$$

$$c_{4i-1} = \frac{\theta_{T_{i+1}}(s_{4i-3} + s_{4i-2}) - \theta_{T_i}(s_{4i-1} + s_{4i})}{(s_{4i-3} + s_{4i-2}) - (s_{4i-1} + s_{4i})} \quad (45)$$

$$a_{4i} = \frac{\theta_{T_i} - \theta_{T_{i+1}}}{((s_{4i-3} + s_{4i-2}) - (s_{4i-1} + s_{4i}))(s_{4i-1} - s_{4i})} \quad (46)$$

$$b_{4i} = \frac{2(\theta_{T_{i+1}} - \theta_{T_i})s_{4i}}{((s_{4i-3} + s_{4i-2}) - (s_{4i-1} + s_{4i}))(s_{4i-1} - s_{4i})} \quad (47)$$

$$c_{4i} = \theta_{T_{i+1}} + \frac{(\theta_{T_i} - \theta_{T_{i+1}})s_{4i}^2}{((s_{4i-3} + s_{4i-2}) - (s_{4i-1} + s_{4i}))(s_{4i-1} - s_{4i})} \quad (48)$$

As can be seen, the structure of the equations is similar to the equations corresponding to the isolated curve. The heuristic process is also very similar, but more stitching points are considered.

4.4 Obtaining the final solution

As explained in Section 3.3, the entire section of the road is divided into smaller segments and the proposed method is used to obtain a sequence of curves for each segment separately. In the last step, all the individual solutions must be assembled to obtain the entire section. This can be easily done since consecutive individual solutions share the same tangent. Thus, the heading of this tangent is calculated by averaging the headings obtained for the two consecutive solutions. Figure 7 shows this step. All the initial and final points of the individual adjustments were initially marked with a spot. After the merging process was carried out, the intermediate tangent was merged and the spots were removed.

4.5 Computer program

A computer program was developed for the proposed method in Visual Basic for Applications. This program determines the initial heading profile and also assists the user in detecting and fitting all the geometric sequences. Finally, it merges all the individual pieces and shows the horizontal alignment.

5 DISCUSSION

The results obtained by the proposed method are considerably more accurate than the results obtained by other methods, such as the curvature-based one. The heading parameter allows the use of certain relationships between geometric features that are not available when other parameters are used.

5.1 Estimating the horizontal alignment for complex geometries

The heading profile is much more readable than the curvature profile and it does not require any smoothing. The proposed method can be applied to some geometric layouts that could not be fitted with other methods. Figure 10 shows one example. This horizontal layout is composed of a sequence of several curves without tangents. Several previous methodologies were not able to find a solution while other methods needed smoothing, which might lead to hiding short geometric elements or to introducing non-existent spiral transitions. The new method does not require smoothing; all the geometry elements, even short ones, can be identified.

As discussed in Section 3.2, flat circular curves have small curvatures that can be easily overlooked in the presence of noisy data – particularly if the curve has a small deflection angle. The opposite may also happen when the noise of the



Figure 8 Example of a curve with a low deflection angle. This curve is hardly detected by other methodologies, but easily found with the one presented in this paper.

curvature profile is confused with a small curvature. As the result, a non-existing curve may be added or an existing one removed.

Use of headings mitigates and in many cases eliminates the above difficulty. A curve, regardless of its radius or its length, always introduces a visible change in the heading direction. Figure 8 shows an example of a low-deflection angle curve. Although the horizontal curve is hardly detected, the change in the heading direction is obvious. Figure 9 shows the curvature and heading profiles for a sequence of tangent-circular curves. The radius of the circular curve is 200 m, which is a medium value. The initial data set of points was configured to simulate data collection by a human user, so it displays some random error. Points are separated at a 1 m interval, while the standard error of all points is considered to be 1 cm. As can be seen, the noise of

the curvature profile considerably masks the change of curvature introduced by the circular curve. Hence, a curvature-based methodology would not detect this geometric element. On the other hand, the noise level of the heading profile is similar to the curvature profile, but the change in the heading direction is considerably higher. Thus, both the geometric elements are easily discernible.

One of the most important advantages of the proposed method is that it detects the number of geometry components and estimates their parameters. The obtained solution is much more accurate than the solutions obtained by other methods. Figure 10 shows the horizontal alignment obtained by two different methods: the curvature-based method presented by Camacho et al. (2010) and the proposed method. The primary cause of the poor performance of the

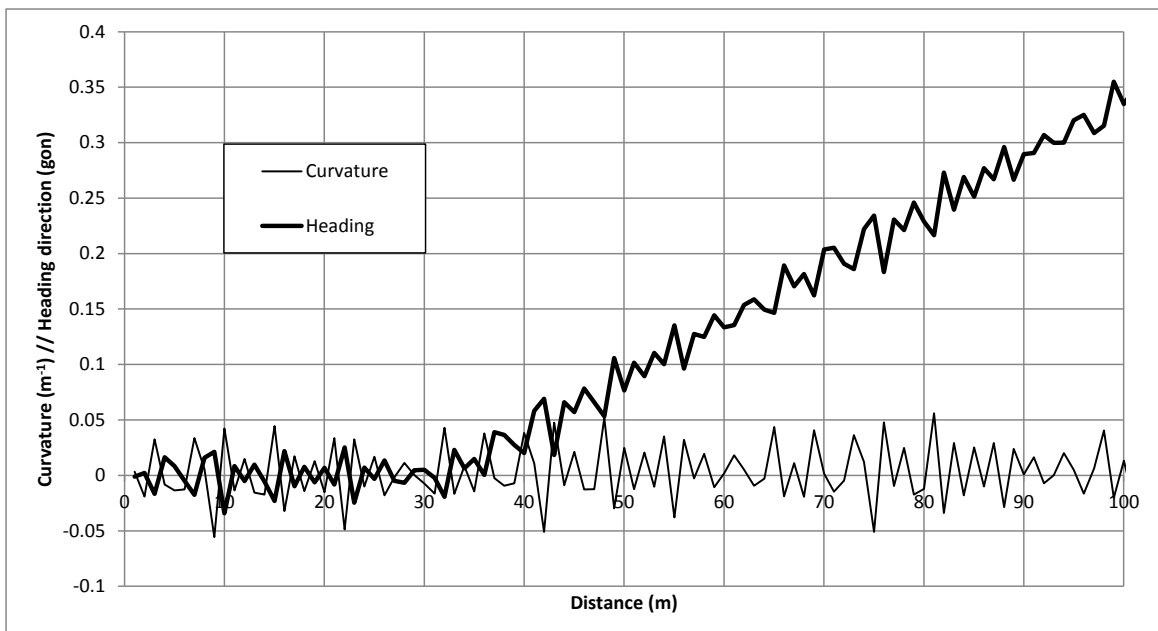


Figure 9 Curvature and heading profile for a tangent-circular curve section.

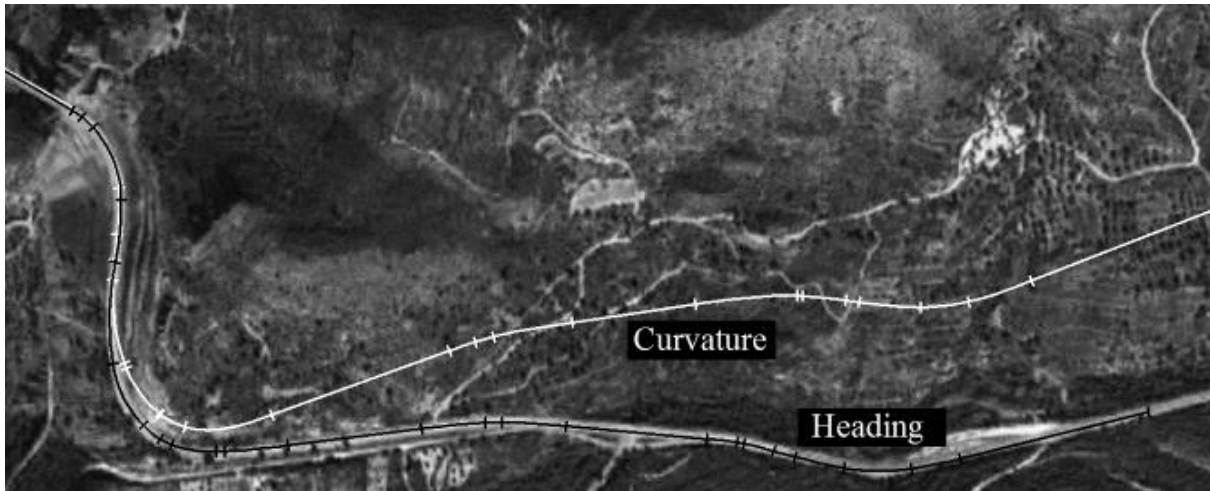


Figure 10 Horizontal alignment fitted by means of the curvature (white) and the heading profile (black).

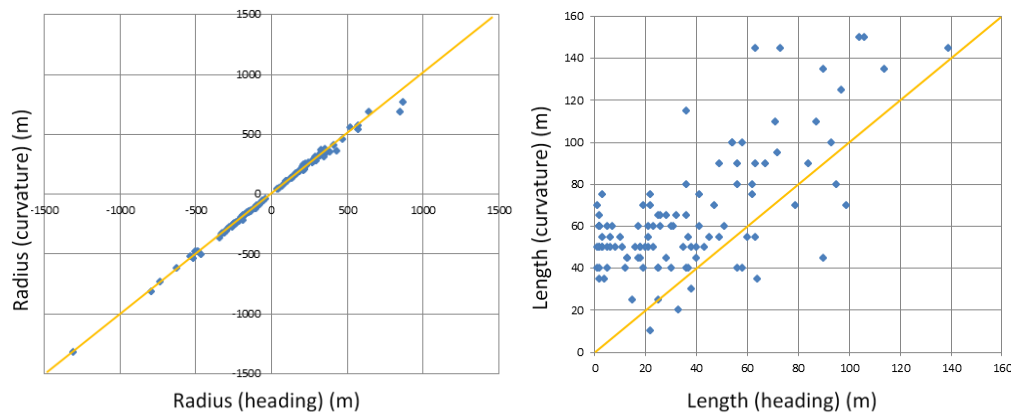


Figure 11 Comparison of the radii and lengths estimated for circular curves with the proposed and curvature-based methods.

other method is incorrect number of geometric elements that leads to accumulation of the location error.

5.2 Comparison to a previous method

Several curvature-based methodologies employ user-defined thresholds for detecting the existence and position of different geometric elements. The resulted solutions may depend on these thresholds. Moreover, it is common than the user-defined thresholds are suitable for a certain range of geometry characteristics and are not suitable for other cases leading to incorrect solutions.

A comparison of radii and lengths of circular curve obtained with the curvature-based method presented by Camacho et al. (2010) and the proposed method was performed. A set of 200 isolated, horizontal curves were randomly extracted from 10 two-lane rural highways in Spain. Figure 11 shows the comparison of the results from the two methods (estimated radii and lengths of the selected curves). As can be seen, the radii obtained with the two methodologies are almost identical, while their lengths are significantly different. In this case, the lengths estimated

with the curvature-based method tend to be higher than those obtained with the proposed method. This discrepancy is caused primarily due to an error in estimating the curve lengths with the curvature-based method.

5.3 Accuracy of the results

The heuristic process used for determining the best location of s_i stitching points evaluates all possible solutions before the final solution is selected based on minimizing the fitting error. The average distance between data points - one meter - is sufficiently precise to obtain accurate estimates of the horizontal alignment. Figure 12 shows the comparison between the estimated and actual geometry of the road alignment. The horizontal curves were correctly detected except one curve composed of two consecutive curves and a very short intermediate tangent. The estimated geometry is sufficiently close to the actual geometry for the purpose of evaluating local curvature from the safety point of view.

The accuracy of the results depends on selected Δs . In this case, $\Delta s = 1$ m, is acceptable for safety and mobility-related analysis that requires curve radius and length. A lower Δs

should be used, such as 1 mm if the estimated alignment is need for the road redesign. Additional steps are needed to accomplish a higher accuracy of results are discussed in the next section where the needed future research is postulated.

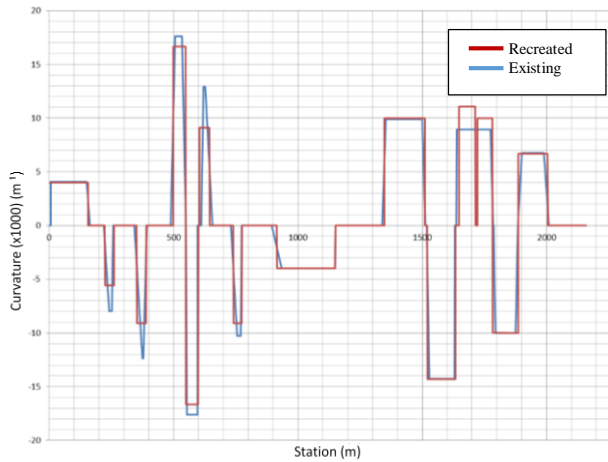


Figure 12 Comparison between the road horizontal alignment obtained by the heading method and the actual alignment obtained from the project.

6 PRACTICAL APPLICATION

In order to show the performance of this methodology, the horizontal alignment of an existing road (CV-35) was obtained. The section goes from station 68+100 to station 86+740.

The road section was manually depicted by one person with Google Earth, thus producing a polyline 18,245 m long,

composed by 2530 points. The user spent 57 minutes on it. Thus, the average distance between points is slightly higher than 7 m. This distance is higher on zones with less curvature, and lower otherwise.

The next step was to transform the polyline into a homogeneous-spaced, (x, y) one. This was performed by a computer program developed by the HERG (Camacho et al., 2010), being immediate. This polyline was introduced in the program to calculate the heading and the horizontal alignment. This process took 92 minutes, performed on a quad-core computer, with 4 GB of RAM. The amount of time is highly dependent on the average curvature of the alignment.

The horizontal alignment is composed by 62 tangents, 85 circular curves and 139 spiral transitions. The largest detected radius was 2242 m, while the sharpest one was only 36 m. It also presented a series of more than 10 consecutive curves. The final road segment length is 18,241 m long, which is only 4 m difference from the original one.

Figure 13 shows the orthoimage of the existing road. Figure 14 shows the intermediate and final results including the initial heading profile, the fitted, and the curvature profile, which is directly related to the horizontal alignment.

7 CONCLUSIONS AND FURTHER RESEARCH

A new method for fitting the horizontal alignment of a road segment was proposed in this paper. Instead of using the curvature as the main input, it uses the heading direction. Abandoning the curvature alleviates the problems caused by noisy measurements and eliminates the necessity of smoothing the profiles before fitting the alignment

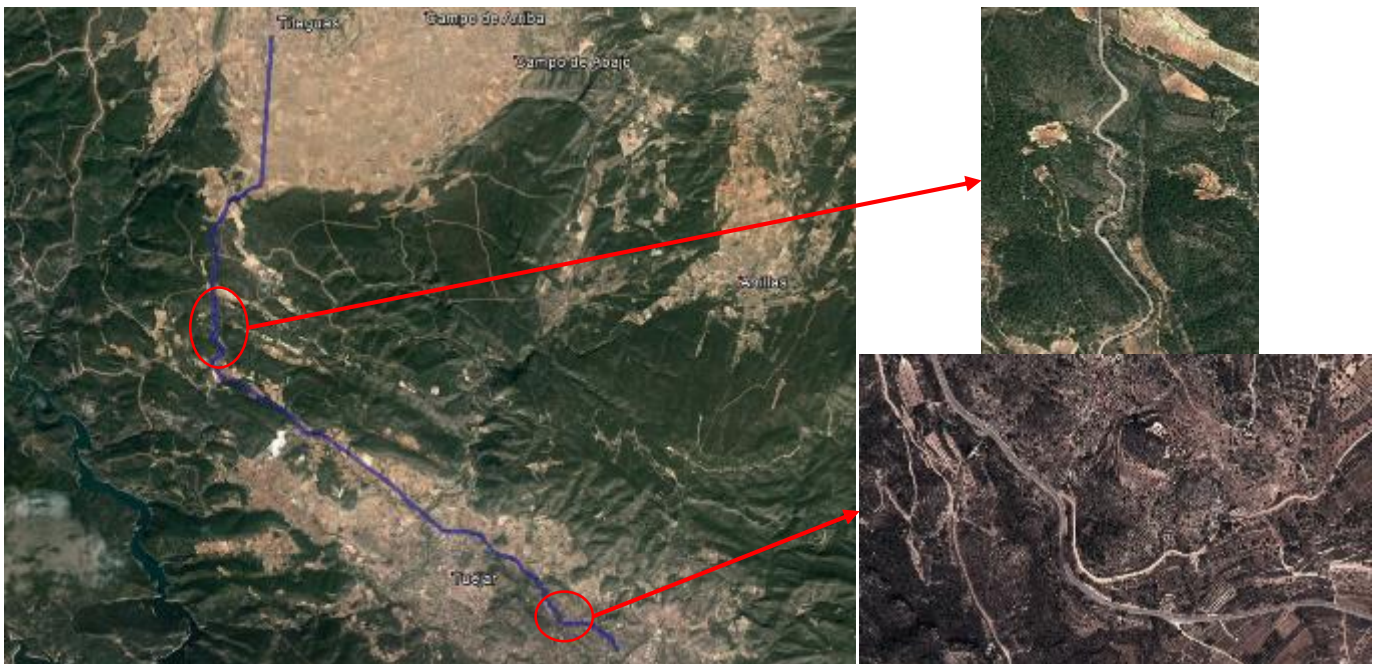


Figure 13 Orthoimage of the road of the case study. Some examples of successions of several curves and flat curves are shown.

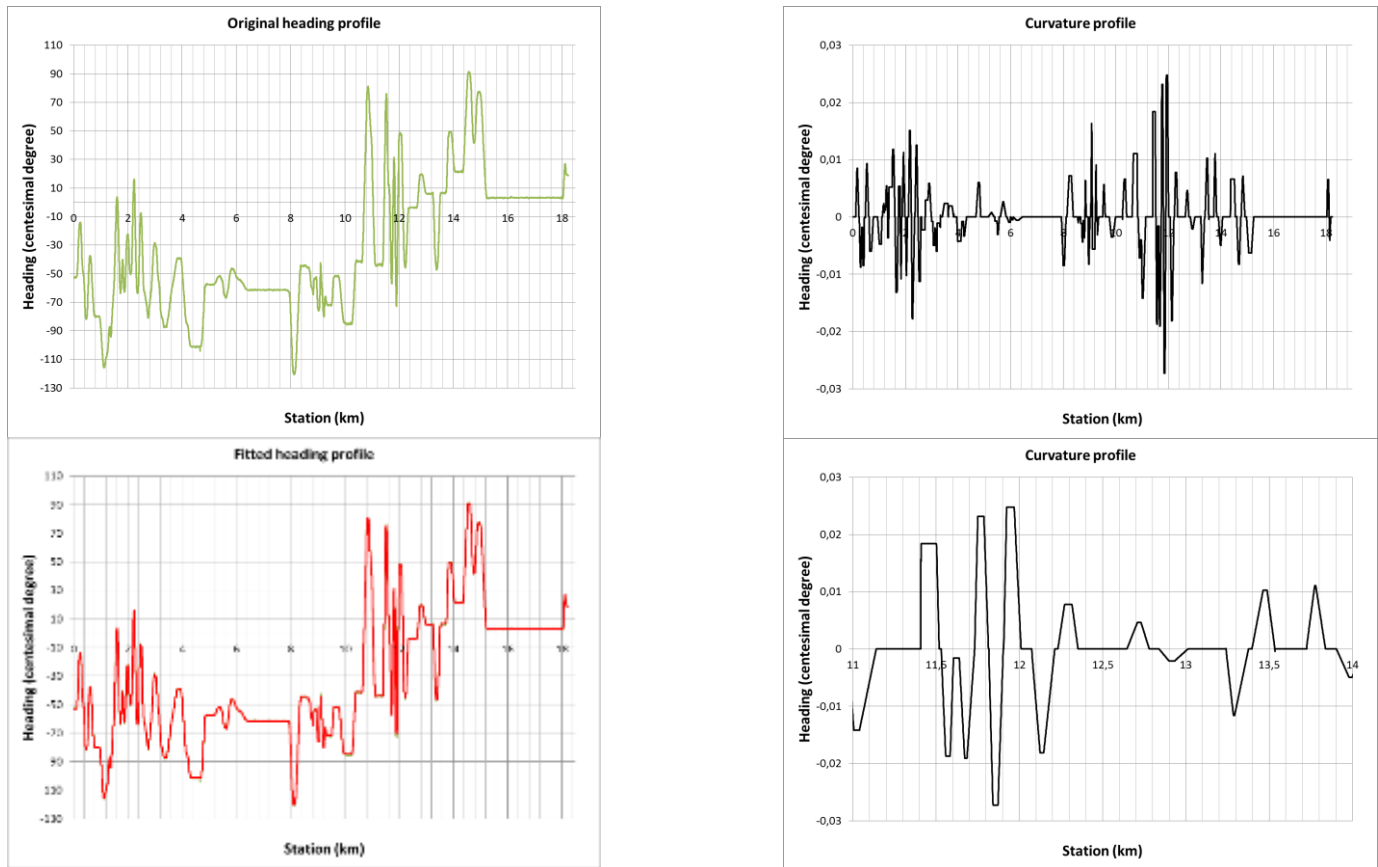


Figure 14 Recreated alignment of the case study. Original heading (top left), fitted heading (bottom left), resulting curvature profile (top right) and a detail of some curves belonging to the most complex zone (bottom right).

component curves. The fitting method uses the geometric properties of the road geometric elements and their relationships. The obtained solution is unique since the user-defined thresholds are eliminated. This new method is practical for complex road alignments. This method is valid for a (x, y) polyline that represents the road centerline. It can be obtained by several methods, highlighting field surveillance, aerial image extraction, GPS-based data collection or automated photographic analysis.

First, the relationship between the curvature and the heading direction was demonstrated, and the most important advantages of this method were explained. These advantages then were used in the paper to fully develop the method and examples were provided.

In the proposed method, each geometric element can be defined by means of the heading direction as a polynomial function: a 0-degree function for tangents, a 1-degree function for horizontal curves and a 2-degree polynomial function for spiral transitions. The most important advantage of the proposed method compared to previous methods is the possibility of using the stitching relationships between consecutive geometric elements. Every point of a road segment must present continuity in its heading direction and in its first derivative (which represents the curvature). Thus,

a set of equations can be set out for each stitching point, leading to an analytical solution to the problem instead of a threshold-based solution. This implies an almost null involvement of the user in the process and that the proposed method would be a powerful tool for very complex horizontal geometries.

A computer application written in Microsoft Visual Basic was developed for the proposed method, and evaluation of the method was conducted. The results confirmed that the proposed method produces the same solution regardless of the assumptions made by different users. Thus, the results generated by this method closely fit the actual road layout.

The proposed method is sufficiently accurate for research and study purposes (i.e., curve negotiation analysis, crash risk determination on curves, operating speed modeling, etc.). On the contrary to most previous methodologies, spiral transitions are not a problem, and complex geometries can be recreated with a minimal involvement of the user. However, the horizontal alignment determined with this methodology is not valid for horizontal alignment redesign. An improvement of the algorithm is needed in order to enhance its accuracy based on the solution presented in this paper. The authors are exploring this topic by adding a Genetic Algorithm that fits the geometry to a set of (x, y)

points. In this case, the solution provided by this methodology is used as the seed solution.

This methodology can also be used for recreating the “operational geometry,” defined as the path followed by actual vehicles. In this case, the initial data set of points may be provided by GPS devices. A polyline that represents the road centerline should be produced by considering the average path of both directions of travel.

Complex horizontal geometries such as compound curves were not discussed here for the sake of brevity. The proposed approach is suitable for such more complex cases and a separate paper is in preparation to discuss them. Vertical alignment was discussed neither. A method with a corresponding algorithm for estimating the vertical alignment should be developed in the future. The proposed methodology is centered on a certain kind of spiral transitions. Some guidelines use different forms of spiral transitions. In such case, the proposed methodology would not be valid. However, the approach might be accurate enough in some cases.

However, the methodology provided does not intend to substitute the previously existing ones, but adding a new tool that may be of interest for some cases where high accuracy at a low effort has to be achieved.

REFERENCES

- Baffour, R. (1997). Global positioning system with an attitude, method for collecting roadway grade and superelevation data. *Transportation Research Record 1592*, 144-150.
- Ben-Arieh, D., Chang, S., Rys, M., and Zhang, G. (2004). Geometric modeling of highways using global positioning system data and B-spline approximation. *Journal of Transportation Engineering 130-5*, 632-636.
- Bosurgi, G. and D’Andrea, A. (2012). A Polynomial Parametric Curve (PPC-Curve) for the Design of Horizontal Geometry of Highways. *Computer-Aided Civil and Infrastructure Engineering 27*, 303-312.
- Cafiso, S. and Di Graziano, A. (2008). Automated in-vehicle data collection and treatment for existing roadway alignment. *4th International Gulf Conference on Roads Compendium of Papers CD-ROM*. Doha (Qatar)
- Cai, H. and Rasdorf, W. (2008). Modeling road centerlines and predicting lengths in 3-D using LIDAR point cloud and planimetric road centerline data. *Computer-Aided Civil and Infrastructure Engineering 23*, 157-173.
- Camacho Torregrosa, F., Pérez Zuriaga, A., and García García, A. (2010). Mathematical model to determine road geometric consistency in order to reduce road crashes. *Mathematical Models of Addictive Behavior, Medicine, and Engineering*. Valencia (Spain).
- Castro, M., Iglesias, L., Rodríguez-Solano, R., and Sánchez, J. (2006). Geometric modeling of highways using global positioning system (GPS) data and spline approximation. *Transportation Research Part C 14-4*, pp 233-243.
- Dong, H., Easa, S., and Li, J. (2007). Approximate extraction of spiralled horizontal curves from satellite imagery. *Journal of Surveying Engineering 133-1*, pp. 36-40.
- Easa, S., Dong, H., and Li, J. (2007). Use of satellite imagery for establishing road horizontal alignments. *Journal of Surveying Engineering 133-1*, pp. 29-35.
- Hans, Z., Souleyrette, R., and Bogenreif, C. (2012). Horizontal Curve Identification and Evaluation. *Iowa State University*
- Hummer, J.E., Rasdorf, W.J., Findley, D.J., Zegeer, C.V. and Sundstrom, C.A. (2010). Procedure for Curve Warning Signing, Delineation, and Advisory Speeds for Horizontal Curves. *Report No. FHWA/NC/2009-07*, available at <http://ntl.bts.gov/lib/38000/38400/38476/2009-07finalreport.pdf>.
- Imran, M., Hassan, Y., and Patterson, D. (2006). GPS-GIS-based procedure for tracking vehicle path on horizontal alignments. *Computer-Aided Civil and Infrastructure Engineering 21*, 383-394.
- Li, Z., Chitturi, M.V., Bill, A.R. and Noyce, D.A. (1997). Automated Identification and Extraction of Horizontal Curve Information from Geographic Information System Roadway Maps. *Transportation Research Record 2291*, 80-92.
- Othman, S., Thomson, R., and Lannér, G. (2012). Using naturalistic field operational test data to identify horizontal curves. *Journal of Transportation Engineering*, pp. 1151-1160
- Pérez Zuriaga, A., García García, A., Camacho Torregrosa, F., and D’Attoma, P. (2010). Modeling operating speed and deceleration on two-lane rural roads with global positioning system data. *Transportation Research Record 2171*, pp. 11-20.
- Price, M. (2010). Under Construction: Building and Calculating Turn Radii. *ArcUser Magazine*, Winter 2010, 50-56.
- Roh, T., Seo, D., and Lee, J. (2003). An accuracy analysis for horizontal alignment of road by the kinematic GPS/GLONASS combination. *KSCE Journal of Civil Engineering 7-1*, 73-79.
- Safahi, Y. and Bagherian, M. (2013). A Customized Particle Swarm Method to Solve Highway Alignment Optimization Problem. *Computer-Aided Civil and Infrastructure Engineering 28*, 52-67
- Tsai, Y., Wu, J. and Wang, Z. (2010). Horizontal Roadway Curvature Computation Algorithm Using Vision Technology. *Computer-Aided Civil and Infrastructure Engineering 25*, 78-88
- Young, S. and Miller, R. (2005). High accuracy geometric highway model derived from multi-track messy GPS data. *Proceedings of the 2005 Mid-Continent Transportation Research Symposium*. Ames, Iowa (EEUU).